Available online at www.sciencedirect.com
ScienceDirect
International Journal of Pharmaceutics 334 (2007) 92–102
INTERNATIONAL JOURNAL OF PHARMACEUTICS
www.elsevier.com/locate/ijpharm

Experimental study of wet granulation in fluidized bed: Impact of the binder properties on the granule morphology

P. Rajniak [a,*], C. Mancinelli [a], R.T. Chern [a], F. Stepanek [b], L. Farber [a], B.T. Hill [a]

[a] *Merck & Co., Inc., WP78-110, P.O. Box 4, West Point, PA 19468-0004, USA*
[b] *Department of Chemical Engineering, Imperial College London, United Kingdom*

Received 28 June 2006; received in revised form 13 October 2006; accepted 17 October 2006
Available online 10 November 2006

Abstract

In this work, the effect of the physicochemical properties of aqueous hydroxypropyl-cellulose (HPC) binder solutions and different pharmaceutical excipients (mannitol and anhydrous $CaHPO_4$) on the agglomeration kinetics and granule properties were investigated. First, a particle size distribution (PSD) analysis together with a detailed analysis of morphological properties of the excipient particles were performed. Second, the viscosity, density, surface tension and size of the spray droplets of binder solutions with different HPC concentrations were determined and wetting characteristics of the binders on the excipients were measured. Third, several fluid bed wet granulation experiments were conducted for pure excipients and their blends with binder solution of different HPC concentrations in a pilot plant Wurster granulator. The observed granule growth for different binder concentrations was a strong function of the binder concentration and the excipient solubility. For mannitol, a significant "coating" period followed by a slow granule growth was observed for the case with the diluted 5% binder. The "coating" period was significantly shorter for the 10% HPC binder and did not exist for the 15% HPC for which immediate and fast granule growth was observed. For anhydrous $CaHPO_4$ (trademark A-TAB), no growth was observed for the 10% HPC binder and a long coating period followed by fast granule growth was observed for the 15% HPC. Simple physically based criteria were also evaluated, which employ the morphological properties of excipients (size and surface roughness) together with physical properties of the used binder for prediction of the coating versus agglomeration regime at given flow conditions (collision velocity). As expected, a preferential coalescence and growth of the mannitol granules from the blend of mannitol + A-TAB was observed. Finally, the mechanical and morphological properties of the produced granules were measured and correlated to the HPC concentration of the binder used in the experiments. A clear correlation between the granule porosity (evaluated by X-ray tomography) and the binder concentration was found for the mannitol granules.

Keywords: Fluid-bed granulation; Coating; Physicochemical properties; Growth mechanism

1. Introduction

Wet granulation is a size enlargement process of converting small-diameter solid particles (typically powders) into larger-diameter agglomerates to generate a specific size, improve flowability and to produce a powder with specific properties such as dissolution rates, granule strength and apparent bulk density (Tardos et al., 1997; Iveson et al., 2001).

According to the operating conditions and the physicochemical properties of the primary particles and binder solution, the evolution of granule properties during granulation is controlled by three processes: coating, growth (agglomeration) and attrition (breakage). During coating, a liquid binder solution is sprayed onto the powder to form a layer of liquid surrounding a particle. This mechanism is observed when the wetted particles become dry before their collision or when the cohesive strength between the wetted particles is weaker than the breakup forces induced by particle–particle collisions in the fluidized bed. During agglomeration, large particles or granules are produced by smaller particles adhering to one another via liquid bridges. Liquid bridges are formed as wetted particles coalesce. Strong solid bridges that hold a granule together develop from the liquid bridges during the subsequent drying step. General reviews signifying the interest of wet granulation were published recently (Iveson et al., 2001; Litster et al., 2004; Boerefijn and Hounslow, 2005; Cameron et al., 2005; Reynolds et al., 2005). It has also

* Corresponding author. Tel.: +1 215 652 0655; fax: +1 215 652 2821.
E-mail address: pavol_rajniak@merck.com (P. Rajniak).

0378-5173/$ – see front matter © 2006 Elsevier B.V. All rights reserved.
doi:10.1016/j.ijpharm.2006.10.040

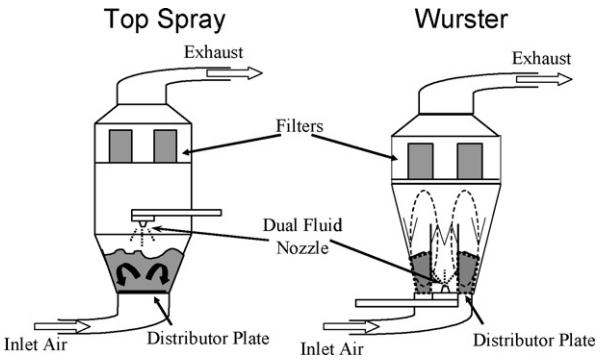

Fig. 1. Comparison of top-spray vs. Wurster fluid-bed granulators.

been suggested that even though some pharmaceutical excipients may be somewhat soluble in the granulating liquid, the polymeric binders are still required to assure appropriate granule strength. Recent works (Farber et al., 2003; Bika et al., 2005) show however, that excipients that are strongly soluble in the liquid binder play a major role in the formation and strength of solid bridges inside a granule.

In recent years several experimental studies were performed to investigate the influence of process variables and physicochemical properties on the granulation mechanisms (Bouffard et al., 2005; Cryer and Scherer, 2003; Pont et al., 2001; Abberger, 2001) and various theoretical models were developed to predict coalescence probability from the physical properties of the primary particles, granules and binder (Liu et al., 2000; Ennis et al., 1991; Adetayo and Ennis, 1997; Stepanek and Rajniak, 2006). These models combine size and morphology of the primary particles/granules with physicochemical properties of the binder and collision velocities of the granules. Most of the models are able to predict whether the granules will stick together or rebound on collision.

Examples of various types of process vessels used in granulation processes include pan, drum and fluidized beds. The main advantage of a fluid-bed granulator is that it is a gentle, tunable and robust process during which many steps (pre-blending, granulation, drying) can be performed in the same piece of equipment. Usually, no milling is required after granulation. Other advantages are usually indicated to be the milder process conditions and product granules with higher porosity and narrower size distribution (Boerefijn and Hounslow, 2005; Bouffard et al., 2005; Cryer and Scherer, 2003; Pont et al., 2001; Abberger, 2001; Guignon et al., 2003; Panda et al., 2001). Two typical set-ups of fluid-bed granulators operating in the bottom-spray versus the top-spray batch mode are compared in Fig. 1. Powder is initially charged into the fluid-bed system. Air is then forced into the granulator at the bottom of the column. A fine mesh/screen keeps powder from leaving at the bottom, while filters at the top of the column allow air to pass, but keep solid particles from escaping. Once the powder is fluidized (and mixed if appropriate), a binder agent is pumped through atomization nozzles and added to the fluid bed in the form of fine droplets. The addition of the binder begins the coating and agglomeration process. When the granules have grown to an appropriate size or the target quantity of binder has been added to the bed, the binder solution flow rate is terminated and the granules are then allowed to dry during the drying phase as air is continually being passed through the system. Relatively new is to employ the Wurster unit, frequently used for coating, for granulation (Shelukar et al., 2005). The Wurster unit operation has the potential to provide better control of the granulation process, granules with more uniform drug distribution and with tighter particle size distribution (PSD). The regular circulation pattern also promotes uniform distribution of binder spray throughout the powder and thereby uniform granulation. Also important are the capabilities for on-line control of granule size and for the scale-up of the granulation process using chemical engineering principles.

This work is focused on experimental investigation of the impact of physicochemical properties of aqueous HPC binder solutions and morphological properties of primary particles on the agglomeration kinetics and granule properties of different pharmaceutical excipients (mannitol and A-TAB) in the Wurster fluidized bed granulator. Simple physically based criteria are also tested, which combine the morphological properties of excipients (size and surface roughness) together with physical properties of the used binder for prediction of the coating versus agglomeration regime at given flow conditions.

2. Theoretical

Ennis et al. (1991) published their landmark paper on the importance of the force balance between binder viscosity and particle inertia (expressed in a critical Stokes number) for successful coalescence. They considered the collision of non-deformable, elastic granules completely covered with liquid layers at the surface. More recently Liu et al. (2000) extended the model of Ennis et al. (1991) by including granule deformation behavior during collisions. In this model, coalescence of two surface-wet granules is assumed to occur when the kinetic energy of impact is fully absorbed through viscous dissipation in the liquid layer and plastic deformation of the bulk granules. The coalescence model gives conditions for two types of coalescence. Type I coalescence occurs when granules coalesce by viscous dissipation in the surface liquid layer and before their surfaces touch:

$$\text{Type I coalescence}: \quad St_v = \frac{8\tilde{m}u_0}{3\pi\mu\tilde{D}^2} < \ln\left(\frac{\lambda}{h_a}\right) \tag{1}$$

Type II coalescence occurs when granules are slowed to a halt during rebound, after their surfaces have made contact. For primary particles with negligible permanent deformation the condition is as follows:

$$\text{Type II coalescence}: \quad St_v < 2\ln\left(\frac{\lambda}{h_a}\right) \tag{2}$$

The condition for rebound (i.e. coating) of colliding non-deformable particles is then:

$$\text{Rebound}: \quad St_v > 2\ln\left(\frac{\lambda}{h_a}\right) \tag{3}$$

where St_v is the viscous Stokes number and $\tilde{m}$ and $\tilde{D}$ reduced particle mass and diameter, u_0 velocity of collision, μ the binder viscosity, and λ is thickness of binder layer on the solid surface with asperity (roughness) h_a.

During early stages of the fluid-bed granulation process originally dry particles pass through the spray-zone and are wetted by the binder droplets, which are generally much smaller than the primary particles (Boerefijn and Hounslow, 2005). We propose a simple extension of the above model also for collisions of primary particles only partially covered by a single binder droplet or by several droplets. One droplet of the binder with volume v creates a spherical cap on the solid surface. Relations for calculations of the base diameter d_{cap} and height h_{cap} of the cap with the wetting angle θ are (de Ruijter et al., 1999):

$$d_{cap} = 2\sqrt[3]{\frac{3v\phi}{\pi}} h_{cap} = d_{cap}\frac{1-\cos\theta}{2\sin\theta} \tag{4}$$

where

$$\phi = \frac{(1+\cos\theta)\sin\theta}{(1-\cos\theta)(2+\cos\theta)}$$

Further we assume that the height of the cap can be replaced by the height of a short cylinder having the same volume and diameter:

$$h = \frac{4v}{\pi d_{cap}^2} = \lambda_{min} \tag{5}$$

In other words, $\lambda = h = \lambda_{min}$ is the average minimum thickness of the binder layer on the solid surface to be used in criteria (1) or (2) for successful coalescence of primary particles partially covered by the binder. Note that the thickness increases with the droplet volume v and with the wetting angle θ.

Once formed and grown to a certain size, granules either survive further particle–particle or particle–wall collisions or break. Tardos et al. (1997) proposed a simple criterion for the granule breakage. They defined a dimensionless Stokes number for deformation St_{def} and assume that breakage occurs if

$$St_{def} = \frac{\tilde{m}u_0^2}{2\tilde{D}^3\tau_Y} > St_{def}^* \tag{6}$$

where τ_Y is a characteristic strength of the granule and St_{def}^* is a critical value of the Stokes number. For example, assuming that the wet granule is a very concentrated slurry of the binder and the original particles and neglecting the apparent viscosity, the characteristic strength for the wet granule can be approximated by the yield strength Y_d. Different models (crush strength model, recrystallized bridge model, autoadhesion model) for calculation of the solid granules strength are reviewed in Bika et al. (2005). In traditional granulation theory, it is assumed that a binder such as a polymer is required to hold particles together once granules form in the granulator and are dried. However, it has been shown (Farber et al., 2003; Bika et al., 2005) that excipients strongly soluble in the liquid binder solution system also play a major role in the formation and strength of solid bridges inside a granule.

3. Experimental

3.1. Materials

Narrow sieve cuts of mannitol (Pearlitol SD-200, Roquette Pharma, Lestrem, France), anhydrous $CaHPO_4$ (A-TAB, Innophos, Cranbury, NJ, USA) and their blends were the starting powders used for granulation experiments. Hydroxypropylcellulose (HPC) binder solutions (5, 10, 15, 20, 25, 30%, w/w) were prepared by adding HPC-SL powder (Nisso Soda Co. Ltd., Tokyo, Japan) to de-ionized water under constant stirring. The solution was gently stirred overnight to allow hydration and degassing.

3.2. Particle size distribution and morphology of solids

Particle size distribution (PSD) analysis of raw materials and granules was performed using the (Sympatec GmbH, Clausthal-Zellerfeld, Germany) analyzer combining (Helos) laser diffraction system in combination with (Rodos) dry powder dispersion and (Vibri) oscillating feed systems. Low pressure of the inlet air was used for the analyses to minimize impact of the granules attrition. A detailed analysis of morphological properties (mean gyration radius, aspect ratio, surface roughness) was performed based on images of primary particles using a scanning electron microscope (Quanta 200, FEI Co., Hillsboro, OR, USA). A high resolution desk-top microcomputed tomography system (SkyScan-1072, Aartselaar, Belgium) was also employed for morphological analysis of granules.

3.3. Surface tension, viscosity, density and droplet size of binders

Surface tension was measured using the plate method (Tensiometer K12, Krüss GmbH, Hamburg, Germany) and the dynamic viscosity was measured by an automated dynamic shear rheometer with cone-plane geometry (Rheometer AR-1000, TA Instruments, New Castle, DE, USA). Solution density was obtained by precisely weighing 10 cm^3 of solution. Droplet size distribution was measured using a laser size analyzer (Spraytec, Malvern Instruments Ltd., Malvern, UK). A drop shape analyzer (DSA-10, Krüss GmbH, Hamburg, Germany) was used for measurement of the wettability of binders with different HPC concentrations. The equipment employs the direct measurement of a liquid drop spreading on the mannitol or A-TAB tablets prepared using the automatic press at compaction pressure of 187.3 MPa.

3.4. Equipment and granulation

The experimental apparatus was a commercial fluid-bed processor (Glatt GPCG3, Glatt GmbH, Binzen, Germany) equipped with the Wurster insert and operated in a bottom-spray batch mode. Before entering the powder bed the fluidizing air flow rate is measured by mass flow meter and preheated. The air distributor is a stainless steel perforated plate with two different meshes and is used to distribute the heated air flow rate, which

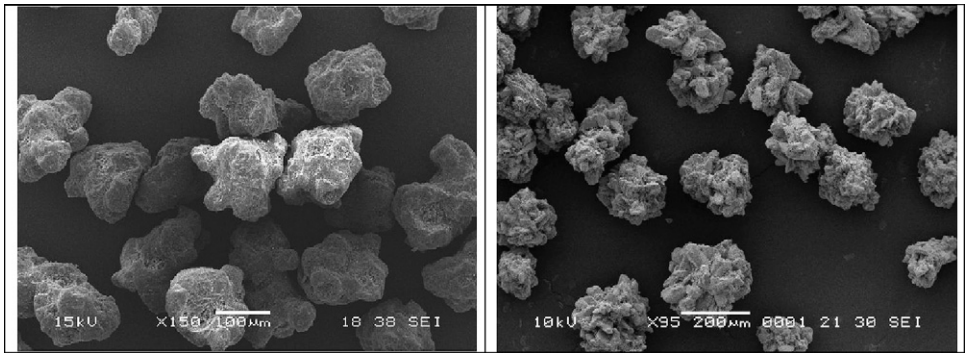

Fig. 2. SEM images of primary particles of mannitol (left) and A-TAB (right).

is greater in the central tube than in the periphery. This assures a regular circulation pattern of the particles. Binder solution is delivered to the powder bed from below through a two-fluid Schlick nozzle fed by a peristaltic pump from a reservoir positioned on a balance. The liquid flow rate is controlled by the pump revolution setting and by the continuous record of reservoir weight. The atomizing air flow rate is controlled by needle valve and measured by a mass flowmeter. The atomizer is an upward facing nozzle and is located in the inner tube in the bed. The air and liquid flow rates, temperatures and pressure drop were monitored during granulation.

3.5. Characterization and chemical analysis of products

During granulation, samples of powder/granules from the fluid bed were taken at every 5 min for off-line measurement of PSD and bulk and tapped densities. In-process growth samples were not dried prior to particle size characterization, however, the final time point was dried prior to characterization as a result of normal process operation. Previous experience has shown that there is little or no impact of drying the in-process granule samples (in a vacuum oven) prior to particle size measurement. It is recognized that there is a possibility for attrition to occur during characterization. For this reason, particle size analysis using the Sympatec laser diffraction system was conducted at the lowest possible dispersion pressures (0.5 bar g) while ensuring adequate presentation of granules to the laser field, and this pressure was held constant throughout all the experiments. In order to understand or to explain some phenomena, chemical analysis (assay) of different samples obtained during the run and at the end of granulation was performed. Sieve fractions were analyzed for dibasic calcium phosphate (CaHPO4,

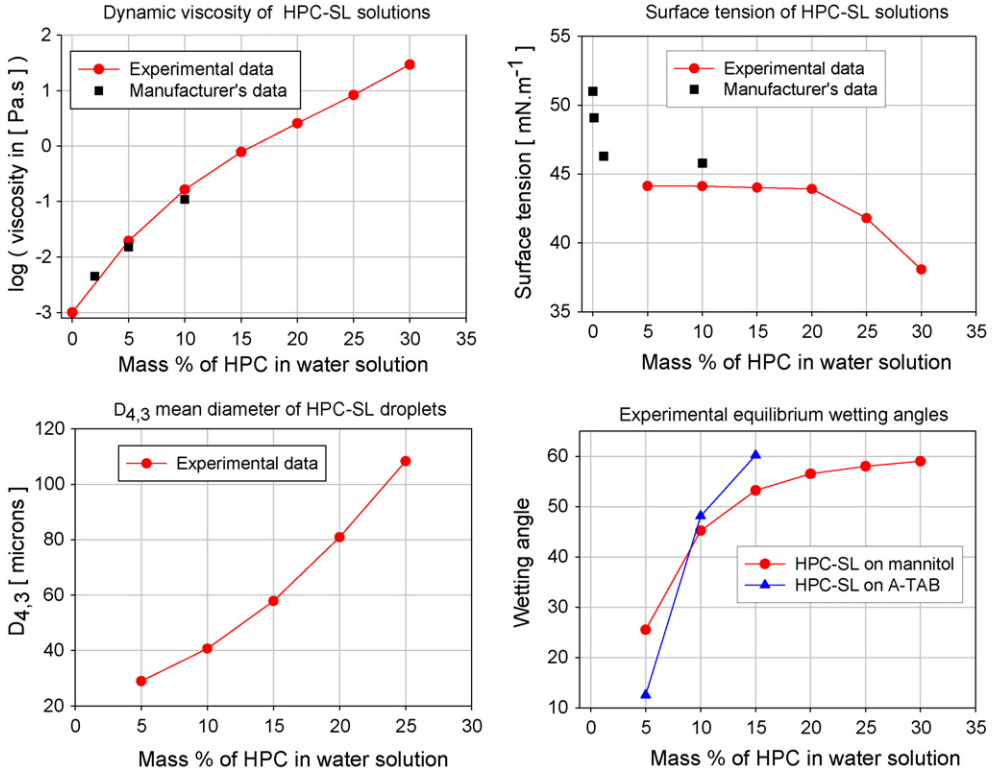

Fig. 3. Basic physical properties for HPC solutions, mannitol, and A-TAB.

Table 1
Summary of basic experimental conditions in Wurster granulator

Experiment #	Solid	HPC concentration (%)	Mass of solid (g)	Mass of added HPC (g)	Rate of binder addition (g/min)	Bed temperature (°C)	Air flow rate (cfm)
1	Mannitol	5	920	80	10.9	20.0	50–60
2	Mannitol	10	920	80	14.6	20.6	50–70
3	Mannitol	15	920	80	11.0	22.4	50–70
4	A-TAB	10	920	80	16.7	19.9	50–80
5	A-TAB	15	920	80	12.5	20.6	50–70
6	Mannitol + A-TAB	10	866	75	14.3	18.9	50–80
7	Mannitol + A-TAB	15	920	80	9.8	20.7	50–70

A-TAB) using a titrimetric assay according to the official USP monograph. Samples were analyzed for mannitol by using ion chromatography with amperometric detection on a Dionex Chromatography system. Mannitol was quantified relative to an external mannitol standard (100% purity, USP).

4. Results and discussion

4.1. Input parameters for the analysis

A sieve fraction of mannitol with average diameter $D = 120\ \mu m$ was used for experiments with pure mannitol. Slightly larger sieve cuts of primary particles of mannitol and A-TAB, with average diameter $D = 152\ \mu m$, were used for experiments with pure A-TAB and 50/50 blend (w/w) of mannitol and A-TAB. Scanning electron microscopy (SEM) images of both primary particles are compared in Fig. 2. Both materials have irregular shape. A-TAB particles have a very rough surface. Asperity (surface roughness) of the primary particles, $h_a = 3.5\ \mu m$ for mannitol versus $h_a = 6.1\ \mu m$ for A-TAB, was estimated by the detailed morphological analysis (Stepanek et al., 2006; Stepanek and Rajniak, 2006). Solubility of the mannitol is 1 g in 5.5 cm^3 of water solution, A-TAB is insoluble in water.

Experimental data of the dynamic viscosity, surface tension and size of the spray droplets are presented in Fig. 3 together with equilibrium wetting angles of binder solutions with different HPC concentration on the mannitol and A-TAB surfaces. Each experimental point represents a mean value from two independent experiments. The binder solution viscosity, equilibrium wetting angle and droplet size increased greatly with the HPC concentration in the range of 5–30% of HPC. On the other hand, the surface tension of different binders is almost constant in the range 5–20% HPC. The limiting wetting angle is higher for mannitol than for A-TAB at 5% HPC. However, at 10% HPC it is already slightly higher for A-TAB and at

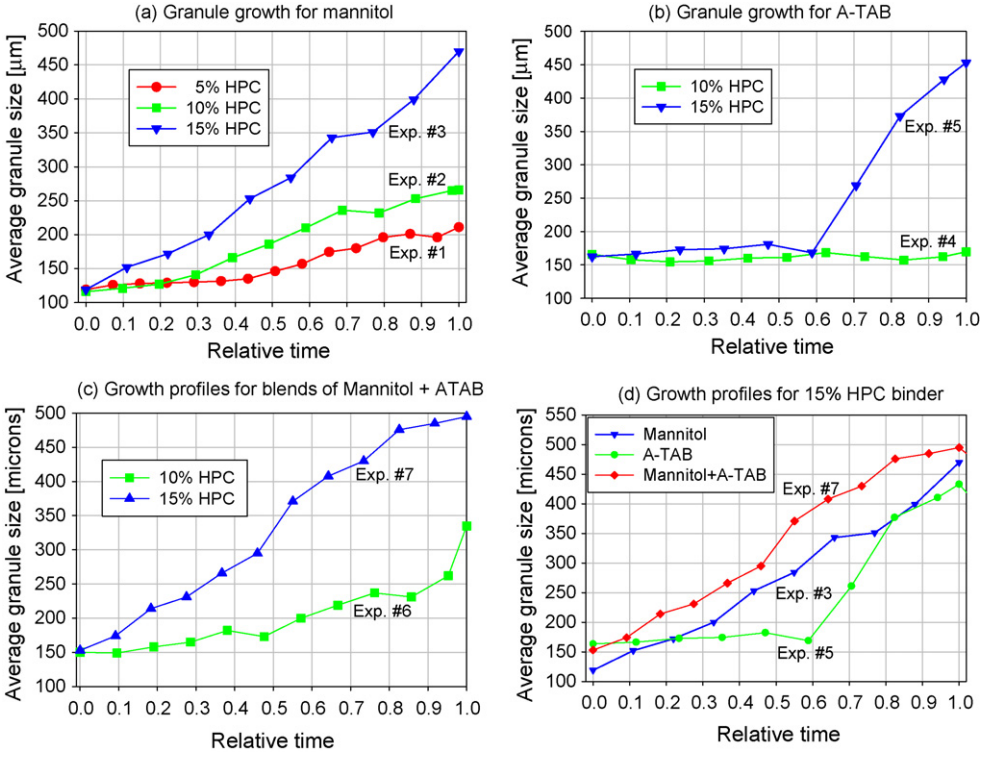

Fig. 4. Comparison of growth profiles for mannitol, A-TAB with HPC binders.

15% HPC the limiting wetting angle is significantly higher for A-TAB than for mannitol.

4.2. Granulation experiments

Experimental conditions of different wet granulation experiments in the Wurster granulation unit are summarized in Table 1.

The goal was to keep constant total material balance of mannitol and HPC and as similar hydrodynamic conditions as possible. Dry mass of HPC added is 8% (80 g in 1000 g batch). This amount was chosen based on previous product development experience and was not deemed to be unnecessarily high based on the growth profiles and final particle size distributions. The flow rate of the fluidizing air was gradually increased during experiments to maintain good and consistent flow pattern. Product samples were taken during the experimental runs and used for the PSD evaluation. Granule growth profiles are shown in Fig. 4 as a function of the relative time = time/duration of experiment. Average granule size represents the volume mean diameter of granules. Amount of the added HPC is the same at the same relative time. Binder addition was chosen as a consistent temporal unit of measure, since the total duration of experiments depends on the binder solution concentration.

The observed granule growth for different binder concentrations was a strong function of the binder concentration and the excipient surface roughness and solubility. Generally, faster growth of the granules was observed with more concentrated binder. In experiments with pure mannitol (Fig. 4a) long coating period (45% of relative time) with no growth was observed for 5% binder. The coalescence starts only after creating a binder layer with a thickness sufficient for successful collision. For 10% binder the coating period is shorter (∼20% of relative time) and it does not exist for 15% binder where the coalescence starts immediately because the binder droplets are much larger and more viscous. In experiments with pure A-TAB (having significantly rougher surface and negligible solubility in water) no growth was observed for the 10% HPC binder and a long coating period followed by fast granule growth was observed for the 15% HPC (Fig. 4b). Finally, in experiments with 50/50 (w/w) blends of mannitol and A-TAB growth profiles similar to the growth profiles for pure mannitol were observed (Fig. 4c). Similar growth profile for pure mannitol and 50/50 blend of mannitol and A-TAB is illustrated in Fig. 4d.

4.3. Comparison with physically based criteria

Viscous Stokes number, the binder layer thickness and the surface asperity were evaluated for experiments #1–5 together with criteria (2) or (3) which define conditions for coalescence or rebound. These criteria combine the morphological properties of excipients (size and surface roughness) with physical properties of the binder and can be used for a simple prediction of the coating versus agglomeration regime at given flow conditions (collision velocity). All properties are summarized in Table 2.

Symbols in Table 2 represent: C_{HPC} = concentration of HPC in the binder solution having dynamic viscosity μ, $D_{4,3}$ = De Broukere mean diameter of one binder droplet which creates on the solid surface a spherical cap with base diameter d_{cap}, height h_{cap} and wetting angle θ, λ_{min} is the average minimum thickness of the binder layer on the solid surface defined by expression (5), $\tilde{m}$ and $\tilde{D}$ are reduced particle mass and diameter, and h_a = asperity (roughness) of the solid surface.

Mean values of the droplet size, the particle size and the asperity were used for evaluation rather than distributions, since a narrow sieve fraction of both A-TAB and mannitol primary particles was used in the experiments. After introduction of parameters from Table 2 into criterion (2) we get conditions for coalescence:

- For mannitol:
  - For 5% HPC collision is successful if $u_0 < 0.04$ m/s;
  - For 10% HPC collision is successful if $u_0 < 2.3$ m/s;
  - For 15% HPC collision is successful if $u_0 < 18$ m/s.
- For A-TAB:
  - For 10% HPC collision is successful if $u_0 < 0.48$ m/s;
  - For 15% HPC collision is successful if $u_0 < 6.4$ m/s.

The coating operation regime is predicted for early stages of experiment #1 with 5% HPC binder solution, because the agglomeration would be successful only for very low collision velocities which are unlikely in the spraying zone of the Wurster unit. The less strict condition for experiment #2 can explain the shorter coating period shown in Fig. 4a. On the other hand, the granulation regime is predicted for the experiment with 15% HPC for which collisions are successful even at very high collision velocities.

Analogous conditions for successful collisions are more strict (3–5 times lower feasible collision velocities) for A-TAB particles as a consequence of the higher surface roughness of this excipient. It can partially explain different growth profiles for the A-TAB with no growth at 10% HPC and significant coating period at 15% HPC shown in Fig. 4b. However, we consider that another contributing factor is the insolubility of the A-TAB in water. In traditional granulation theory, it is assumed that a binder such as a polymer is required to hold particles together

Table 2
Summary of basic properties for evaluation of criteria (1)–(3)

Experiment #	C_{HPC} (%)	μ (Pa s)	$D_{4,3}$ (μm)	d_{cap} (μm)	h_{cap} (μm)	θ (°)	λ_{min} (μm)	$\tilde{m}$ (μg)	$\tilde{D}$ (μm)	h_a (μm)
1	5	0.0195	30	68	7.7	25.8	3.9	0.5	60	3.5
2	10	0.1643	40	73	15.2	45.5	8.1	0.5	60	3.5
3	15	0.7620	60	102	25.5	53.1	13.8	0.5	60	3.5
4	10	0.1643	40	71	15.9	48.1	8.4	1.5	76	6.1
5	15	0.7620	60	96	27.9	60.2	15.5	1.5	76	6.1

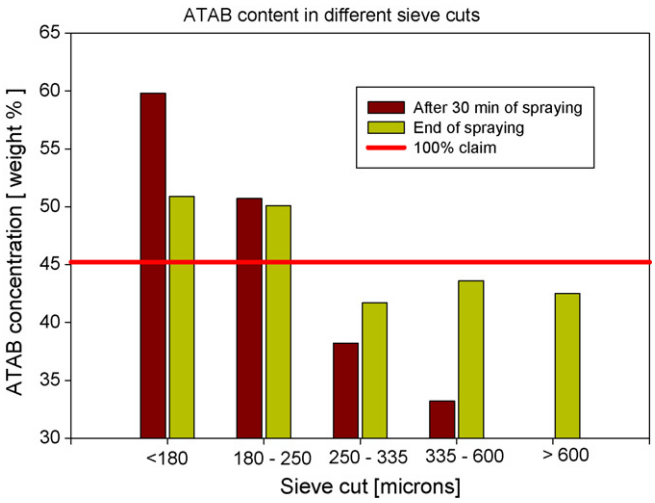

Fig. 5. A-TAB distribution vs. sieve fraction in granules with mannitol.

once granules form in the granulator and are dried. However, it has been shown (Farber et al., 2003; Bika et al., 2005) that excipients strongly soluble in the liquid binder solution system also play a major role in the formation and strength of solid bridges inside a granule.

The systematic experimental study of physical properties of typical excipients, active substances and binder solutions used for granulated products combined with physically based criteria helps in understanding and predicting the operation regimes during coating or granulation processes. Other solid + binder systems will be studied in the near future in an effort to generalize existing observations. The application of the theory in this contribution is qualitative and applied only to early stages of the coating/granulation process. Mean values of the droplet size, the particle size and the asperity height are used for evaluation rather than distributions, since a narrow sieve fraction of both A-TAB and mannitol primary particles was used in the experiments. Simplified criteria allow for computation of approximate ranges of collision velocities between primary particles for successful collisions. The approximate ranges are used for qualitative comparison of granulation potential of different solid + binder combinations and predicting the preferential growth of one component from a blend of different solid components. To make this approach more useful for simulation and prediction of the whole granulation process, it will be necessary to combine it with computational fluid dynamics (CFD) models allowing calculation of profiles of collision velocity in the granulator. The agglomeration theory must also be extended to include collisions between a particle and a granule and between granules. Mathematical models for prediction and scale-up of fluid-bed granulation processes combining CFD with population balancing and with agglomeration theory are under development (Rajniak et al., 2005, 2006; Stepanek and Rajniak, 2006).

4.4. Granule properties

For experiments with 50/50 (mass basis) blends of mannitol and A-TAB we can assume that both components behave independently (ideal mixture). Consequently, the growth for 15% HPC binder should be controlled at early time points by the

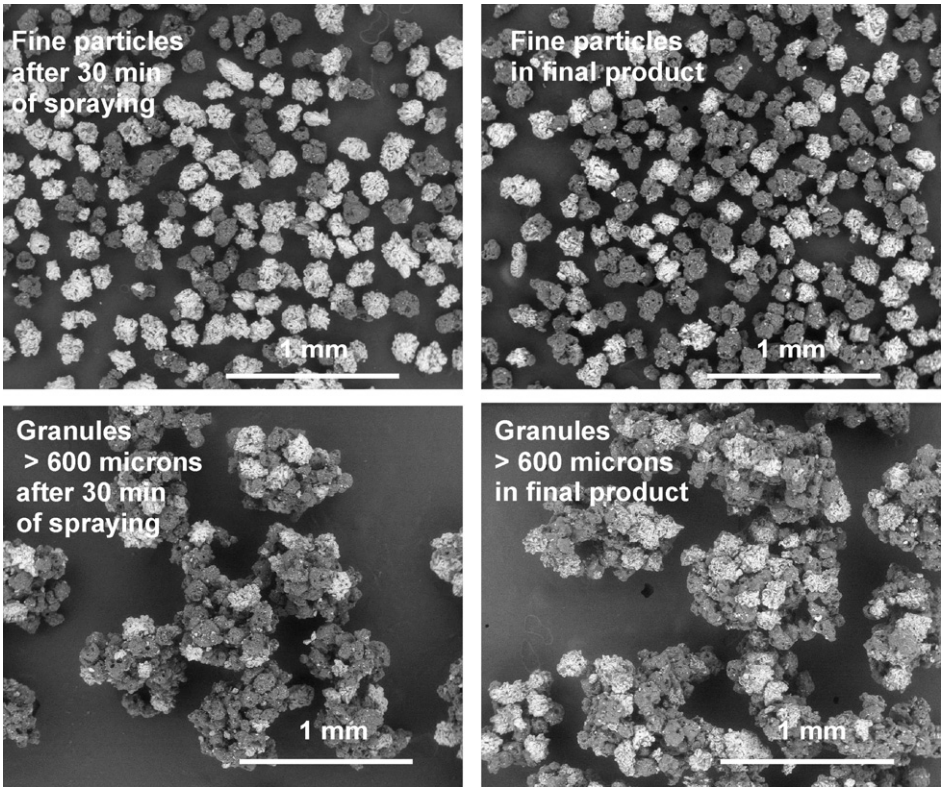

Fig. 6. SEM images of fines vs. large granules at different stages of process (mannitol is dark and A-TAB is white).

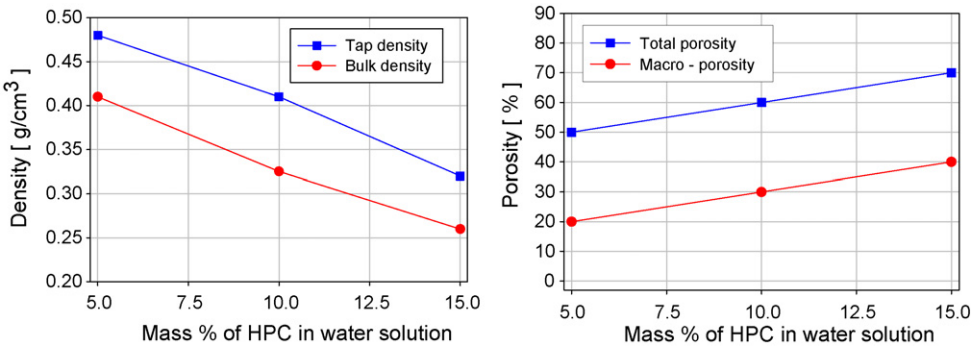

Fig. 7. Granule porosity and density as function of the binder concentration.

coalescence of mannitol particles only and after ∼30 min will the A-TAB particles also coalesce. This hypothesis was tested by chemical analysis of different sieve fractions of samples taken after 30 min of spraying and after 55 min (final product). Results are presented in Fig. 5. Note that no granules >600 μm were produced after 30 min of spraying. The chemical analysis shown in Fig. 5 confirms the above assumption of preferential growth of the mannitol-enriched granules at early stages. However, the granules do not contain exclusively mannitol but also some entrapped A-TAB particles. These results are also supported by SEM images of primary particles and granules at different stages of the process (30 min versus end of granulation) shown in Fig. 6. Porosity of mannitol granules was evaluated using reconstructed cross-sectional images. XRCT software was used to both reconstruct images and evaluate the porosity. Morphology of the granules is strongly dependent on the binder concentration. Total porosity (summation of the mannitol internal porosity and granule porosity) and granule porosity (macroporosity) estimated from the images is reported in Fig. 7. With increasing HPC concentration the porosity of the granules increases. The reverse trend is expected and observed from the dependence of the granules bulk density (both tap and pour) on the binder concentration, as also shown in Fig. 7.

Morphological analysis of mannitol + A-TAB granules is presented in Fig. 8. All methodologies can nicely distinguish between A-TAB, mannitol and voids. SEM image on left side was done with backscattered electrons, and brighter particles are A-TAB. In the central XRCT image, A-TAB particles are much darker than mannitol particles. Finally, on the XRCT cross-section, A-TAB is almost black and mannitol is gray.

Morphological analysis of mannitol granules is presented in Fig. 9. Images are grouped in columns for each HPC concentration and are (top to bottom): SEM (side view), XRCT (side view, transmission), XRCT-reconstructed cross-section (used also for evaluation of porosity in Fig. 7). Granules produced with 5, 10 and 15% of HPC were imaged. The more porous structure of the granules with 15% HPC supports the theoretical prediction of faster growth (see criteria in Section 4.3) without need of complete coating of primary particles. On the other hand, denser granules are produced with 5% HPC when the coating period is needed. All granule properties clearly correlate with the binder concentration, with physical properties of the solid + binder system, with the granule growth dependencies and with theoretical predictions of the coating versus granulation regime.

4.5. Comparison of experimental and computed granule microstructures

Virtual granules (Stepanek and Ansari, 2005; Stepanek, 2004) have been generated by random packing of primary particles possessing the same morphological characteristics as mannitol particles (Stepanek et al., 2006). The virtual granules were generated so as to have porosity matching that of physical granules shown in Fig. 9, i.e. approximately 20%, 30%, and 40% (referring to granule porosity, i.e. not counting the internal porosity of mannitol particles). The virtual granules are shown in Fig. 10 in a similar format as that of Fig. 9, i.e. in a 3D view and as cross-section. By qualitative comparison with actual granules, one can conclude that the virtual granules are realistic models of the real, physical ones. In particular the relationship between

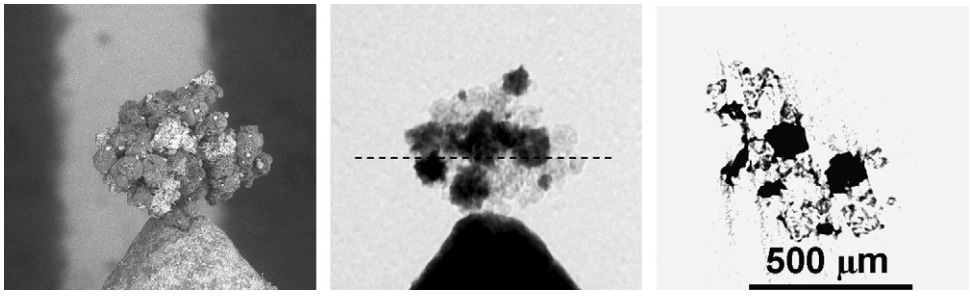

Fig. 8. Morphological analysis of the mannitol/A-TAB granules manufactured with 15% HPC binder.

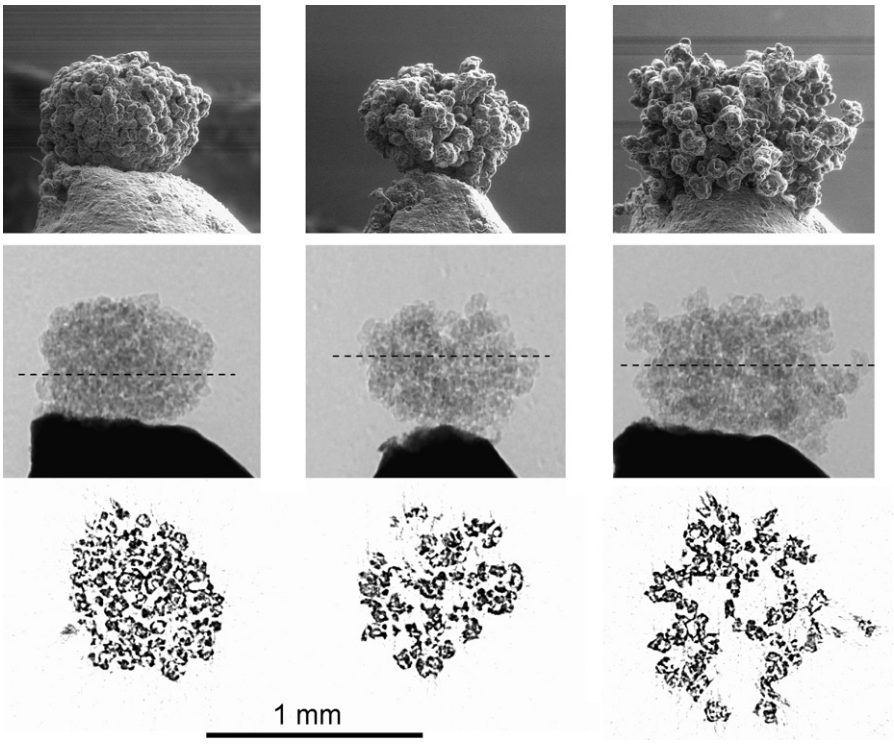

Fig. 9. Morphological analysis of the mannitol granules manufactured with different binders.

internal porosity and external morphology of the granules is well reproduced in the virtual granules—the granules with lowest porosity are nearly spherical and compact, while granules with the highest porosity have a visibly more open, irregular structure with individual particles occasionally "sticking out" of the main granule structure.

Further simulations have been performed in order to illustrate the effect of primary particle morphology on the liquid distribution on the particle surface after contact with a spray of droplets (Stepanek and Rajniak, 2006). The initial conditions (10 randomly deposited liquid droplets) and asymptotic liquid distribution satisfying equilibrium wetting angles of 20° and

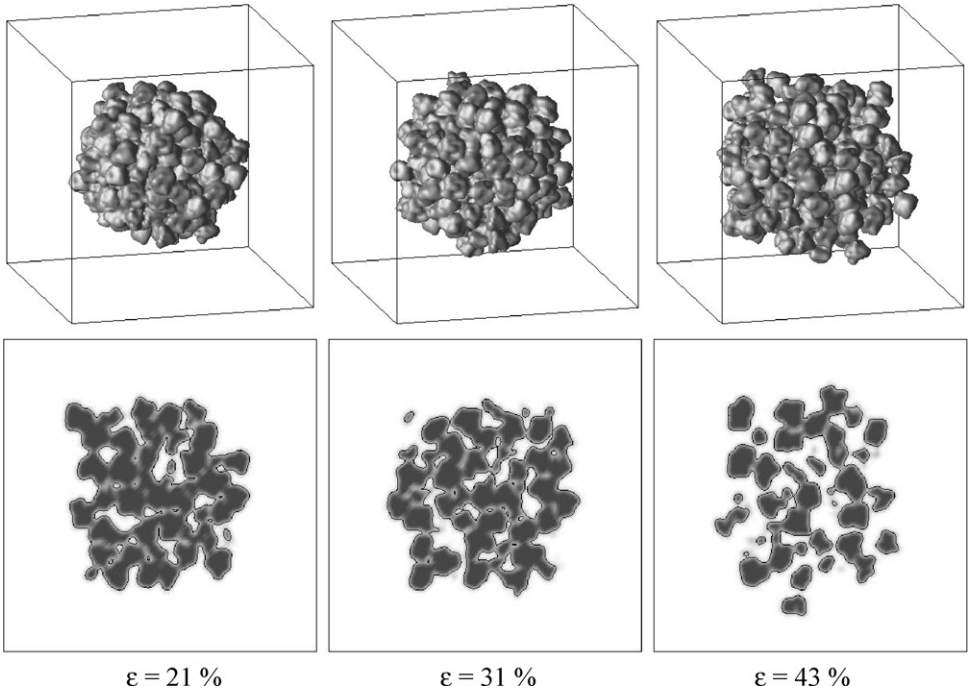

Fig. 10. Virtual granules obtained by random packing of computer-reconstructed mannitol primary particles.

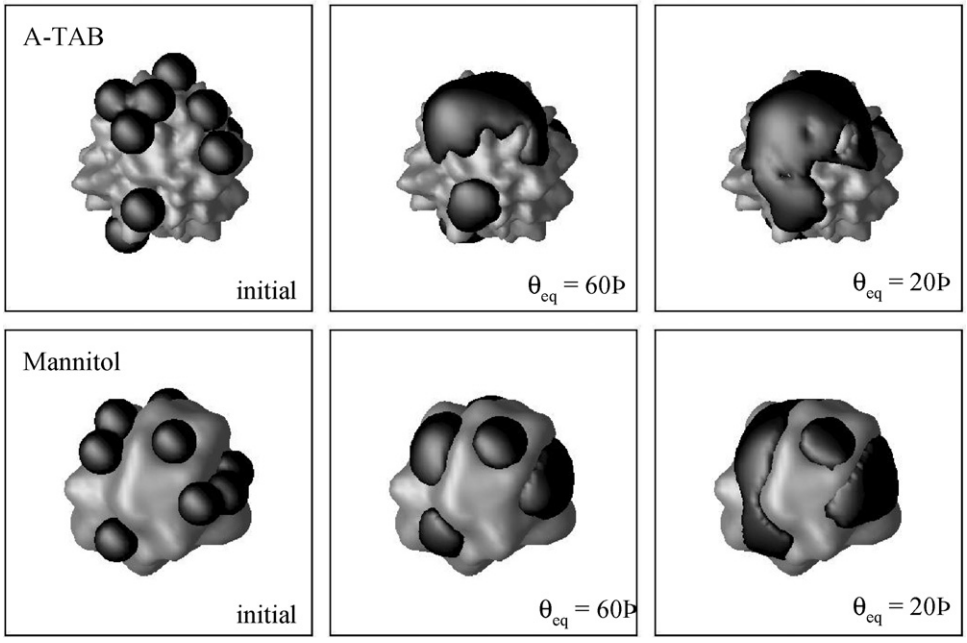

Fig. 11. Computed equilibrium liquid-phase distribution on the surface of mannitol and A-TAB primary particle for two wetting angles: 20° and 60°.

60° (roughly corresponding to 5 and 15% HPC solutions) are shown in Fig. 11 for computer-reconstructed mannitol and A-TAB primary particles. The figure reveals an interesting trend: the fractional surface coverage of the rougher particle (A-TAB) appears to be higher than that of the smoother (mannitol) particle; however, since the total volume of the liquid deposited on the particle was the same in each case, this means that the average thickness of the liquid layer on the A-TAB particle must be lower. As was already discussed in Section 3, this means lower probability of coalescence under otherwise identical conditions, as was indeed observed in the experiments. Another trend revealed by Fig. 11 is that for mannitol, the difference between the fractional surface coverage – and therefore the average liquid thickness – for 20° and 60° is not as profound as for the A-TAB particle. This is also consistent with experimental data: there was a substantial difference between the agglomeration rate of A-TAB particles for 10% (no growth) and 15% HPC (growth after an "induction" period), whereas mannitol particles agglomerated for both concentrations, the only difference was in the rate. A full discussion of the effect of particle morphology on the surface coverage can be found in Stepanek and Rajniak (2006).

5. Conclusions

Physical properties of aqueous HPC binder solutions with different HPC concentrations have a direct impact on the granule growth and granule properties for both tested excipients and their blends.

For mannitol, a significant "coating" period followed by slow granule growth was observed for the case with the 5% HPC binder. The "coating" period was significantly shorter for the 10% HPC binder and did not exist for the 15% HPC for which an immediate and fast granule growth was observed.

For anhydrous $CaHPO_4$ (A-TAB), no growth was observed for the 10% HPC binder and a long coating period followed by fast granule growth was observed for the 15% HPC.

As expected from experiments with pure excipients, a preferential coalescence and growth of the mannitol granules from the blend of mannitol + A-TAB was confirmed by both chemical analysis and SEM imaging.

These regimes are qualitatively predicted using simple physically based criteria, which combine the morphological properties of excipients (size and surface roughness) together with physical properties (viscosity, wetting properties, droplet size) of the used binder. The insolubility of A-TAB in water and resulting weaker bridges likely contribute to generally slower growth for the A-TAB particles.

Mechanical and morphological properties of the produced granules were also measured. A clear correlation between the granule porosity or density and the binder concentration was found for the mannitol granules.

References

Abberger, T., 2001. The effect of powder type, free moisture and deformation behaviour of granules on the kinetics of fluid-bed granulation. Eur. J. Pharm. Biopharm. 52, 327–336.

Adetayo, A.A., Ennis, B.J., 1997. Unifying approach to modeling granule coalescence mechanisms. AIChE J. 43, 927–934.

Bika, D., Tardos, G.I., Panmai, S., Farber, L., Michaels, J.N., 2005. Strength and morphology of solid bridges in dry granules of pharmaceutical powders. Powder Technol. 150, 104–116.

Boerefijn, R., Hounslow, M.J., 2005. Studies of fluid bed granulation in an industrial R&D context. Chem. Eng. Sci. 60, 3879–3890.

Bouffard, J., Kaster, M., Dumont, H., 2005. Influence of process variable and physicochemical properties on the granulation mechanism of mannitol in a fluid bed top spray granulator. Drug Develop. Ind. Pharmacy 31, 923–933.

Cameron, I.T., Wang, F.Y., Immanuel, C.D., Stepanek, F., 2005. Process systems modeling and applications in granulation: a review. Chem. Eng. Sci. 60, 3723–3750.

Cryer, S.A., Scherer, P.N., 2003. Observations and process parameter sensitivities in fluid-bed granulation. AIChE J. 49, 2802–2809.

de Ruijter, M.J., De Coninck, J., Oshanin, G., 1999. Droplet spreading: partial wetting regime revisited. Langmuir 15, 2209–2216.

Ennis, B.J., Tardos, G.I., Pfeffer, R., 1991. A microlevel-based characterization of granulation phenomena. Powder Technol. 65, 257–272.

Farber, L., Tardos, G.I., Michaels, J.N., 2003. Evolution and structure of drying material bridges of pharmaceutical excipients: studies on a microscopic slide. Chem. Eng. Sci. 58, 4515–4525.

Guignon, B., Regalado, E., Duquenoy, A., Dumoulin, E., 2003. Helping to choose operating parameters for a coating fluid bed process. Powder Technol. 130, 193–198.

Iveson, S.M., Litster, J.D., Hapgood, K.B., Ennis, J., 2001. Nucleation, growth and breakage phenomena in agitated granulation processes: a review. Powder Technol. 117, 3–39.

Liu, L.X., Litster, J.D., Iveson, S.M., Ennis, B.J., 2000. Coalescence of deformable granules in wet granulation processes. AIChE J. 46, 529–539.

Litster, J.D., Ennis, B.J., Liu, L., 2004. The Science and Engineering of Granulation Processes. Kluwer Academic Publishers.

Panda, R.C., Zank, J., Martin, H., 2001. Modeling the droplet deposition behavior on a single particle in fluidized bed spray granulation process. Powder Technol. 115, 51–57.

Pont, V., Saleh, K., Steinmetz, D., Hemati, M., 2001. Influence of the physicochemical properties on the growth of solid particles by granulation in fluidized bed. Powder Technol. 120, 97–104.

Rajniak, P., Chern, R., Stepanek, F., Mancinelli, C., 2005. Mathematical modeling of wet granulation: combination of population balances, mesoscale modeling and FLUENT granular model, Paper 369c. In: Proceedings of the AIChE Annual Meeting, Cincinnati.

Rajniak, P., Fox, R.O., Dhanasekharan, K., Stepanek, F., Chern, R., 2006. Solution of population balance equations for wet granulation, CD #2, Paper 4f. In: Proceedings of the World Congress on Particle Technology, Orlando, April 23–27.

Reynolds, G.K., Fu, J.S., Cheong, Y.S., Hounslow, M.J., Salman, A.D., 2005. Breakage in granulation: a review. Chem. Eng. Sci. 60, 3969–3992.

Shelukar, S., Dumont, H., Ho, J., Mancinelli, C., 2005. Process for granulating particles. US Patent Application.

Stepanek, F., 2004. Computer-aided product design: granule dissolution. Chem. Eng. Res. Des. 82, 1458–1466.

Stepanek, F., Ansari, M.A., 2005. Computer simulation of granule microstructure formation. Chem. Eng. Sci. 60, 4019–4029.

Stepanek, F., Rajniak, P., Chern, R., Mancinelli, C., 2006. Modeling of multicomponent granule formation in a wet granulation process. CD #2, Paper 117b. In: Proceedings of the World Congress on Particle Technology, Orlando, April 23–27.

Stepanek, F., Rajniak, P., 2006. Droplet morphologies on particles with macroscopic surface roughness. Langmuir 22, 917–923.

Tardos, G.I., Khan, I.M., Mort, P.R., 1997. Critical parameters and limiting conditions in binder granulation of fine powders. Powder Technol. 94, 245–258.